

# Dynamo Action in a Nearly Integrable Chaotic Flow

Y. Ponty, A. Pouquet, V. Rom-Kedar & P.L. Sulem  
OCA, CNRS URA 1362  
BP 229  
06304 Nice Cedex 04, France

*M.R.E Proctor, P.C Matthews & A.M Rucklidge (eds.)*  
Theory of Solar and Planetary Dynamos, 241-248  
Cambridge University Press (1993).

## Abstract

Dynamo action of a time periodic flow with frequency  $\Omega$ , depending on two space variables, introduced by Galloway & Proctor (1992) is considered when the underlying dynamical system is nearly integrable. Competition between fast and slow dynamos is obtained according to the value of  $\Omega$ . Fast dynamos produce magnetic sheets located in the chaotic regions near the separatrices of the integrable flow. Slow dynamos lead to magnetic eddies which elongate with increasing magnetic Reynolds number  $R_m$  and tend to circumscribe elliptic stagnation points. Sheets and eddies may coexist at moderate  $R_m$ . A heuristic argument based on the Melnikov method is used to characterize the frequencies which maximize the efficiency of fast dynamos.

## 1 Introduction

A simple smooth chaotic flow often used as a candidate for fast dynamos is the “ABC flow”  $\mathbf{u} = (A \sin z + C \cos y, B \sin x + A \cos z, C \sin y + B \cos x)$ , where  $A, B, C$  are non-zero coefficients. This flow only involves one wavenumber, which considerably reduces the number of operations when the induction equation for the magnetic field

$$\partial_t \mathbf{b} = \nabla \times (\mathbf{u} \times \mathbf{b}) + \eta \Delta \mathbf{b} \quad (1)$$

is solved numerically in Fourier space (Arnold & Korkina 1983, Galloway & Frisch 1986). The dynamo problem is however three-dimensional, which limits the Reynolds number to moderate values.

Examples of flows that seem well-suited to probe the large magnetic Reynolds number limit on present-day computers were recently introduced by Galloway & Proctor (1992) who used the fact that flows depending on only two space variables can be chaotic if they are time-dependent. We concentrate here on their “circularly polarized” model (CP)

$$\mathbf{u} = (A \sin(z + \sin \Omega t) + C \cos(y + \cos \Omega t), A \cos(z + \sin \Omega t), C \sin(y + \cos \Omega t))(2)$$

These flows which display large chaotic regions, can be viewed as a modification of the integrable ABC flow corresponding to  $B = 0$ , by the introduction of a time periodic phase. For this velocity, magnetic field modes with wavevectors having the same component  $k_1$  in the  $x$ -direction, evolve independently. Consequently,  $k_1$  can be fixed and the magnetic field computed with a two-dimensional code. For convenience, the  $(y, z)$ -periodicity of the magnetic field is taken as that of the flow. There is no periodicity in the  $x$ -direction and  $k_1$  can be chosen arbitrarily (but non-zero). For  $k_1 = 0.57$ , together with  $A = C = \sqrt{3/2}$  and  $\Omega = 1$ , convincing evidence of fast dynamo was obtained, the magnetic growth rate remaining essentially constant for magnetic Reynolds number  $10^2 \leq R_m \leq 10^4$ . We consider here a similar flow, but in a regime where it is nearly integrable. This is obtained by introducing a small parameter  $\epsilon$  in front of the oscillatory phase of the velocity.

## 2 The dynamical system

The fluid trajectories, to be understood mod  $2\pi$ , obey

$$\dot{y} = A \cos(z + \epsilon \sin \Omega t), \quad \dot{z} = C \sin(y + \epsilon \cos \Omega t) \quad (3)$$

together with  $\dot{x} = A \sin(z + \epsilon \sin \Omega t) + C \cos(y + \epsilon \cos \Omega t)$ . By dividing (3) by  $C$  and rescaling time, it is easily seen that, in addition to the perturbation amplitude  $\epsilon$ , this dynamical system depends on only two parameters, the reduced frequency  $\omega = \Omega/C$  and the ratio  $a = A/C$ . We concentrate here on the case  $a = 1$  for which the unperturbed system has heteroclinic orbits. For convenience, results will be presented in terms of  $\omega$ .

For  $\epsilon = 0$ , system (3) admits two elliptic stagnation points  $(0, \pi/2)$ ,  $(\pi, 3\pi/2)$ , and two hyperbolic ones  $(0, 3\pi/2)$ ,  $(\pi, \pi/2)$ . For  $\epsilon \neq 0$ , the points of zero velocity rotate with angular velocity  $\Omega$  on circle of radius  $\epsilon$ , centered at the stagnation points of the unperturbed problem. Useful insight on the system is provided by Poincaré sections in time (stroboscopic views) at  $t = n2\pi/\Omega$  with  $n \in \mathbb{N}$ . The size of the chaotic zones is as expected monotonically decreasing with  $\epsilon$ , yet exhibits a non trivial dependency with  $\omega$ . Figure 1 shows the section in the  $(x, y)$ -plane, for  $\epsilon = 0.1$ , and various  $\omega$ . The observable chaotic regions are localized along the heteroclinic connections of the unperturbed system, whereas for  $\epsilon = 1$  they cover a large fraction of the domain.

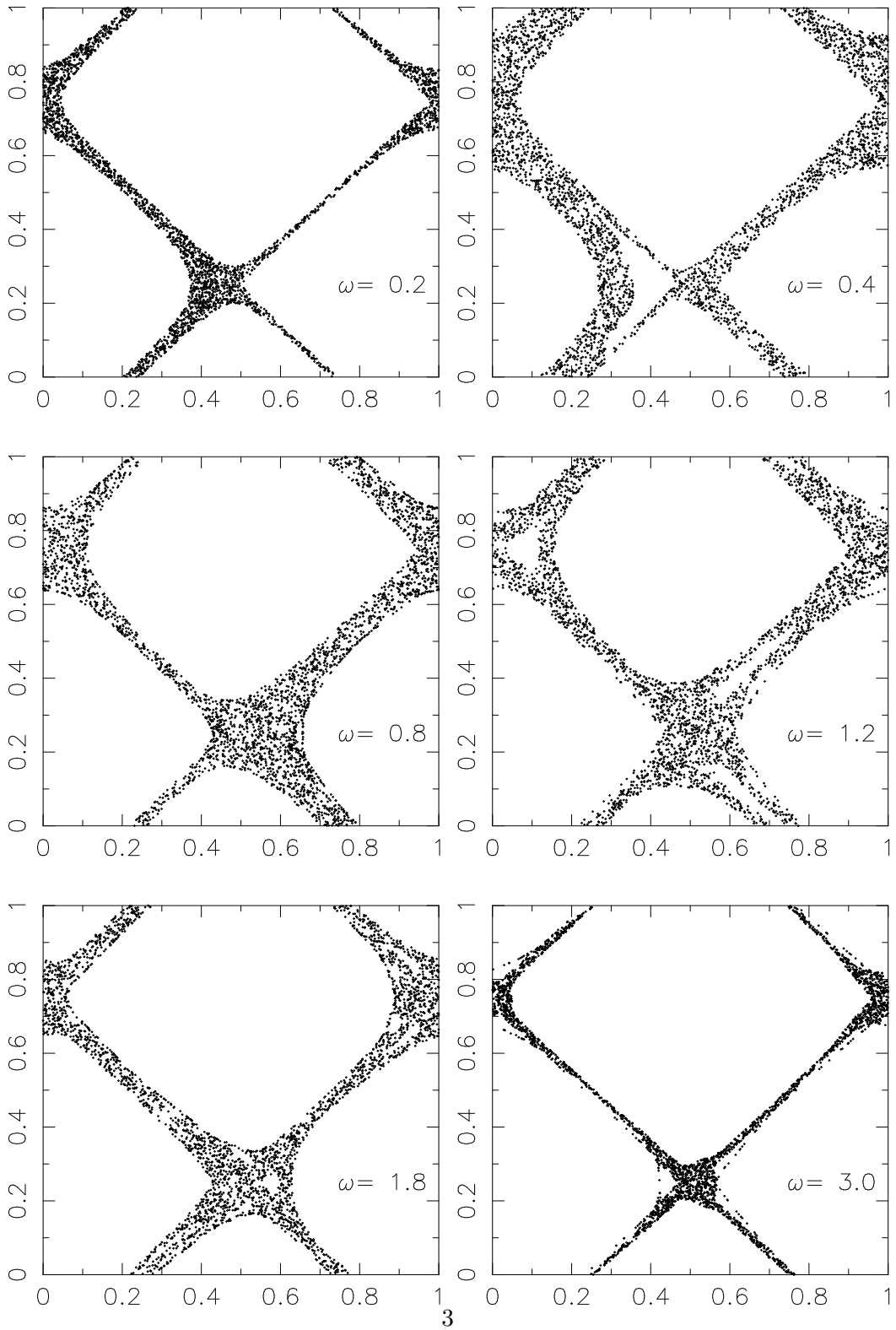


Figure 1: Time Poincaré sections for flow (3), with  $a = 1$ ,  $\epsilon = 0.1$ .

### 3 Dynamo action

The induction equation (1) has been integrated with the above velocity field in the case  $A = C = 1$  and  $\epsilon = 0.1$ . The wavenumber  $k_1$  in the  $x$ -direction was taken equal to 0.57, as in Galloway & Proctor (1992). The magnetic Reynolds number  $R_m = 1/\eta$  was pushed up to  $10^4$  and the reduced frequency  $\omega$  varied from 0 to 3. We observe that as soon as the magnetic Reynolds number exceeds a few units, after a transient, the magnetic energy  $\int \mathbf{b}^2 d\mathbf{x}$  grows exponentially in time with a growth rate  $2\lambda$ . In Figure 2,  $\lambda$  is plotted versus  $R_m$  for various  $\omega$ . For some values, e.g.  $\omega = 0.8$ ,  $\lambda$  tends to saturate at a finite value as  $R_m$  increases, indicating a fast dynamo. In contrast for  $\omega = 0.2$ , the growth rate decreases monotonically for  $R_m > 10$ , at least up to  $R_m = 5000$ . The question arises whether this decay continues for arbitrarily large Reynolds number corresponding to a slow dynamo. It is however not precluded that for any finite non-zero  $\omega$ , a (weak) fast dynamo emerges at large enough Reynolds number. Note that at sufficiently low Reynolds number  $\lambda$  is not sensitive to  $\omega$  since growth rates corresponding to different  $\omega$  fall on the same curve  $\lambda$  versus  $R_m$ . The separation from this common curve occurs at different Reynolds numbers for different frequencies, with a minimum for  $\omega \approx 0.8$ . We interpret this behaviour as resulting from a competition between slow and fast dynamos. Note that for  $\omega = 0.8$ ,  $\lambda$  seems to saturate at a value close to 0.15, only a factor of two below the value obtained for this frequency with  $\epsilon = 1$ .

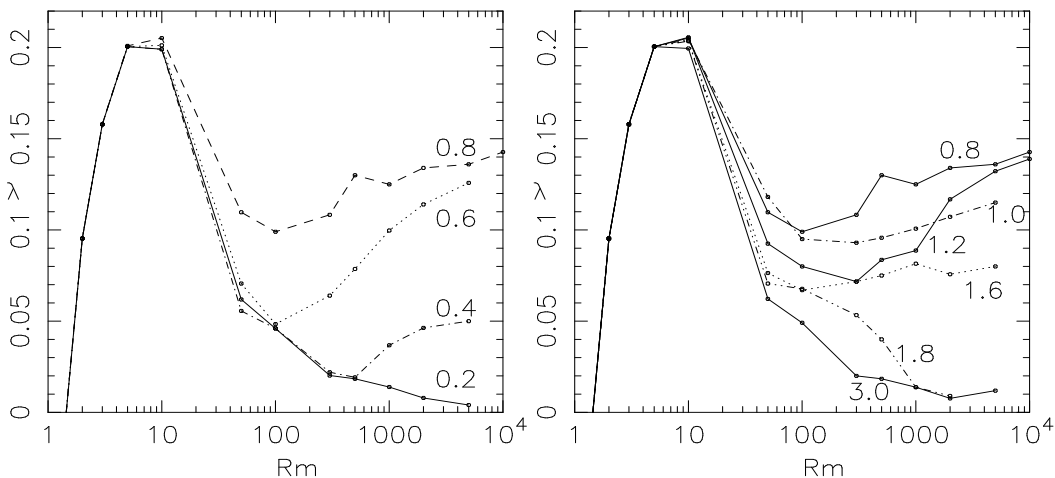


Figure 2: Dynamo growth rate  $\lambda$  versus the magnetic Reynolds number  $R_m$ . Curves are labelled by the corresponding value of  $\omega$ .

The geometry of the magnetic structures are significantly different for fast and slow dynamos. Figure 3 shows the contours of the magnetic field amplitude in the  $(y, z)$ -plane for various  $\omega$  at  $R_m = 2000$ . At  $\omega = 0.8$ , for which the dynamo appears to be fast, the magnetic structures consist essentially of magnetic layers located in the chaotic regions, near the separatrices of the unperturbed system. As  $R_m$  is increased, the thickness of the layers decreases, possibly like  $R_m^{-1/2}$  as suggested by a dominant balance argument between stretching and dissipation. Furthermore, the transverse structure of the layer becomes richer with the formation of secondary maxima, and is reminiscent of the structure of the tangled unstable manifold of (3).

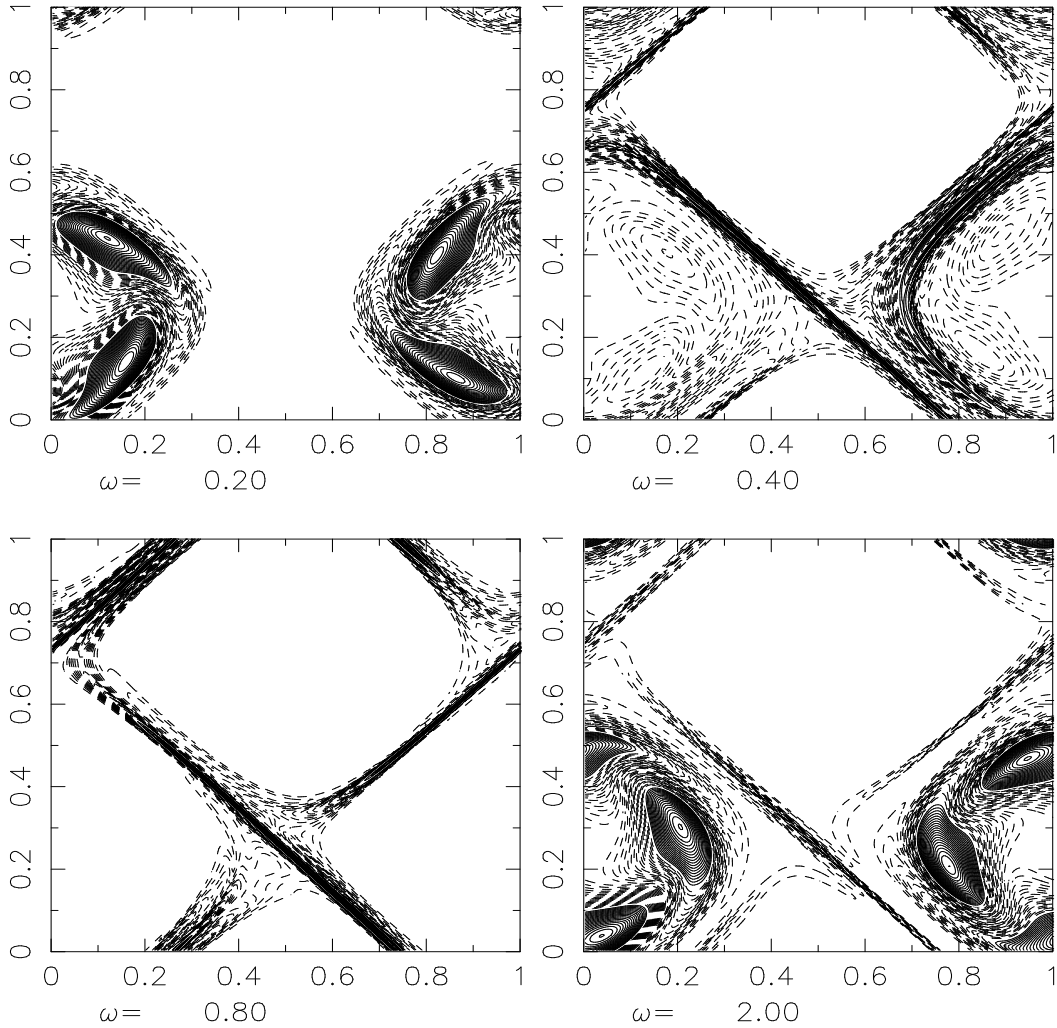


Figure 3: Contours of magnetic field intensity at  $R_m = 2000$ . Dashed lines refer to levels smaller than half the maximum.

For  $\omega = 0.2$ , for which the dynamo appears to be slow, the magnetic field concentrates in “magnetic eddies”, located in non-chaotic regions, close to the resonance bands of system (3). As  $R_m$  is increased, the magnetic eddies, which are rather isotropic at moderate Reynolds numbers, become more elongated and tend to circumscribe the elliptic points. It is noticeable that magnetic eddies, like the resonance bands of (3), appear only in the neighbourhood of zero velocity points rotating in the same direction as the flow particles.

#### 4 Dynamo and chaos: how are they Connected?

We already observed that the dynamo growth rate is sensitive to the velocity frequency. Figure 4 shows this dependency for  $R_m = 1000$  and  $R_m = 2000$ . The central peak, associated with a fast dynamo is maximum at  $\omega \simeq 0.8$  and tends to a fixed form as  $R_m$  is increased. In contrast, the level of the wings decreases in this limit, as expected for a slow dynamo. The question arises how this behaviour is related to the underlying dynamical system.

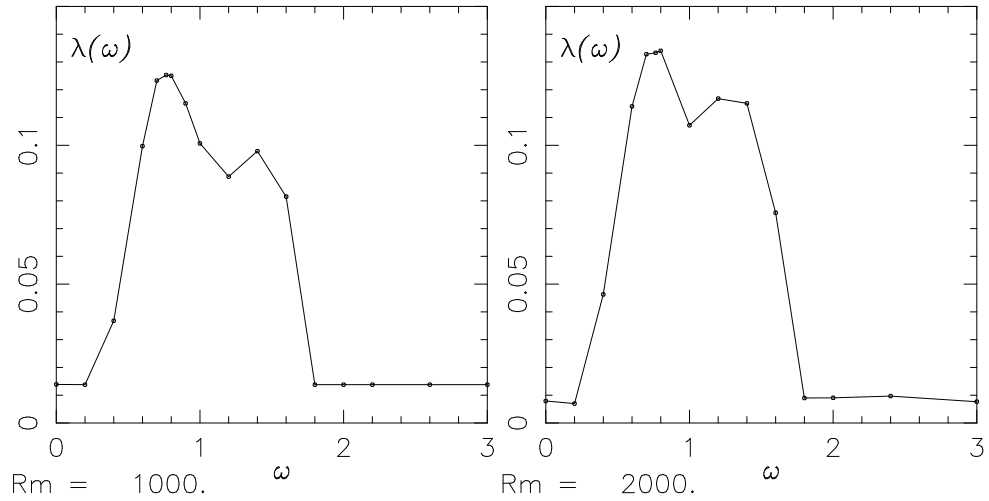


Figure 4: Dynamo growth rate  $\lambda$  versus the reduced frequency  $\omega$  for  $\epsilon = 0.1$ , at  $R_m = 1000$  and  $R_m = 2000$ .

A standard characterization of a dynamical system is provided by Lyapunov exponents, because of the analogy between separation of infinitesimally close fluid particles and stretching of the magnetic field at zero magnetic diffusivity. Figure 5(a) shows the largest Lyapunov exponent  $L$  versus  $\omega$  for the trajectories shown in Figure 1. The correlation between this graph and the dynamo growth rate at large magnetic Reynolds number appears to be weak. This confirms that, in the presence of magnetic diffusion, the rate of stretching alone cannot prescribe the efficiency of the dynamo action. Massive cancellation can indeed take place between magnetic field elements stretched in directions which vary strongly from place to place.

One may suspect that the geometry of chaotic zones of the flow and in particular their extent may affect the efficiency of the fast dynamo action. It was suggested by Leonard *et al.* (1987) and Ottino (1989) that the “extent of chaos” may be estimate using the Melnikov method. This method is a perturbative calculation of the distance between stable and unstable manifolds resulting from perturbation of homoclinic or heteroclinic trajectories. It is classically used to test the existence of transverse homoclinic orbits which imply the presence of Smale horseshoes and their attendant chaotic dynamics (Guckenheimer & Holmes 1983; Ottino 1989).

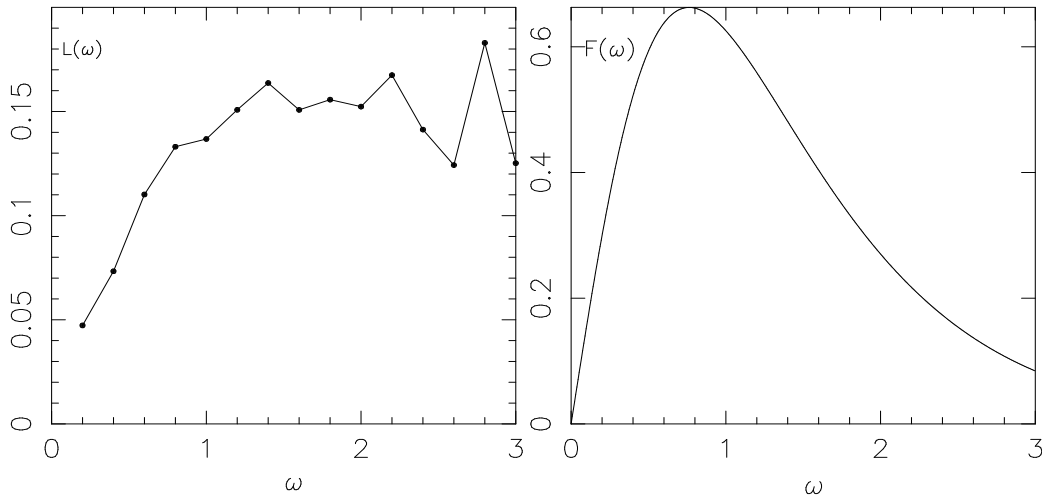


Figure 5: (a) Variation with the reduced frequency  $\omega$  of the maximum Lyapunov exponent  $L$  and (b) of the function  $F$  given in (7) for  $\epsilon = 0.1$ .

By the change of variables  $u = z - \pi/2 + \epsilon \sin \omega \tau$ ,  $v = y + \epsilon \cos \omega \tau$  and  $\tau = Ct$ , and for  $a = 1$ , (3) becomes

$$\dot{u} = \sin v + \epsilon \omega \cos \omega \tau ; \dot{v} = -\sin u - \epsilon \omega \sin \omega \tau . \quad (4)$$

This is the standard form for the implementation of Melnikov method. To leading order in  $\epsilon$ , the distance  $d(\tau_0)$  between the manifolds is proportional to  $\epsilon$  and to the “Melnikov function”. For each of the unperturbed heteroclinic solution  $(u_0^j, v_0^j)$ , where  $j = 1, 2, 3, 4$ , this function reads

$$M^j(\tau_0) = -\omega \int_{-\infty}^{\infty} \sin v_0^j \sin(\omega(\tau + \tau_0)) d\tau + \omega \int_{-\infty}^{\infty} \sin u_0^j \cos(\omega(\tau + \tau_0)) d\tau . \quad (5)$$

After some algebra, we get

$$M^j(\tau_0) = F(\omega) (S_1^j \sin \omega\tau_0 + S_2^j \cos \omega\tau_0) , \quad (6)$$

where  $(S_1, S_2) = (-1, 1), (-1, -1), (1, -1), (1, 1)$  for  $j = 1, 2, 3, 4$  respectively. Furthermore

$$F(\omega) = \omega\pi \operatorname{sech}\left(\frac{\pi\omega}{2}\right) . \quad (7)$$

Quoting Ottino (1989), “we expect that an extreme in  $F(\omega)$  should maximize the extent of chaos”. This function is plotted in Figure 5(b). We observe that the range of frequencies  $\omega$  leading to the largest dynamo growth rates (Figure 4) is located around the maximum of  $F(\omega)$ . We checked that for sufficiently small  $\epsilon$  (typically  $\epsilon < 0.5$ ), this behaviour is essentially independent of  $\epsilon$ .

The Melnikov method has here been used as an heuristic tool to measure the width of the chaotic zones. Further investigations are required to decide whether the location of the maximum dynamo growth rate is indeed correlated with the location of the maximum of the Melnikov function (as found here) or if it is mostly a coincidence. As the next step, we plan to examine the case  $a \neq 1$ , where heteroclinic connections of the unperturbed problem are replaced by homoclinic orbits.

Computations were performed on the CRAY-YMP of the Institut Méditerranéen de Technologie (Marseille).

## References

- [1] Arnold V.I. & Korkina E.I. 1983 The growth of magnetic field in an incompressible flow, *Vestn.Mosk.Univ.Mat.Meckh.* **3**, 43-46 .
- [2] Galloway, D.J. & Frisch, U. 1986 Dynamo action in a family of flows with chaotic stream lines, *Geophys.Astrophys.FluidDyn.* **36**, 53-83.
- [3] Galloway, D.J. & Proctor, M.R.E. 1992 Numerical calculations of fast dynamos for smooth velocity field with realistic diffusion, *Nature*, **356** , 691-693.
- [4] Guckenheimer. J. & Holmes. P. 1983 Nonlinear Oscillations Dynamical System and Bifurcations of Vector Fields, *AppliedMathematicalSciencesSeries* **42**, Springer.
- [5] Leonard, A., Rom-Kedar, V. & Wiggins 1987 S. Fluid mixing and dynamical systems, *Nucl.Phys. B(Proc.Suppl.)* **2**, 179-190.
- [6] Ottino, J.M. 1989 The Kinematics of Mixing: Stretching, Chaos and Transport, *CambridgeTexts inAppliedMathematics*, Cambridge University Press.